University of Wisconsin Milwaukee
UWM Digital Commons

Theses and Dissertations

May 2017

Downstream Predictability of the Path of Severe Wind Producing MCSs Using RUC Analysis Data

Russell Danielson
University of Wisconsin-Milwaukee

Follow this and additional works at: https://dc.uwm.edu/etd

 Part of the Atmospheric Sciences Commons

Recommended Citation
Danielson, Russell, "Downstream Predictability of the Path of Severe Wind Producing MCSs Using RUC Analysis Data" (2017). *Theses and Dissertations*. 1462.
https://dc.uwm.edu/etd/1462

This Thesis is brought to you for free and open access by UWM Digital Commons. It has been accepted for inclusion in Theses and Dissertations by an authorized administrator of UWM Digital Commons. For more information, please contact open-access@uwm.edu.

DOWNSTREAM PREDICTABILITY OF THE PATH OF SEVERE WIND PRODUCING MCSs USING RUC ANALYSIS DATA

by

Russell Danielson

A Thesis Submitted in

Partial Fulfillment of the

Requirements for the Degree of

Master of Science

in Mathematics

at

The University of Wisconsin-Milwaukee

May 2017

ABSTRACT

DOWNSTREAM PREDICTABILITY OF THE PATH OF SEVERE WIND PRODUCING MCSs USING RUC ANALYSIS DATA

by

Russell Danielson

The University of Wisconsin-Milwaukee, 2017
Under the Supervision of Professor Paul Roebber

A method for predicting the track of mesoscale convective systems (MCSs) is developed, based upon meteorological parameters in the path of the systems. Rapid Update Cycle model analysis from the years 2007 through 2011 were used to gather meteorological data for 94 MCS events. An artificial neural network model was developed to predict whether the MCS will track to the "Right", "Left", or stay on its current path. The most important parameters to predict the track of an MCS in this model are precipitable water, most unstable CAPE, 700hPa temperature, surface-500hPa mean wind, low-level equivalent potential temperature difference, and 700-500hPa lapse rate. The model produced a threat score of 0.30 and a Heidke skill score of 0.16 which demonstrates relatively small skill but compares favorably to similar warm season forecasts. When considering the prediction of each class, the model proved to be skillful when predicting "Left" and "Right" classes while it did not skillfully predict the "Middle" class. Sensitivity analysis revealed that surface-500hPa mean wind was the most influential meteorological parameter for forecasting the track of MCSs, with smaller (higher) values giving a greater chance for MCSs to track in the "Middle" and "Right" ("Left"). This relationship may help forecasters improve decision support services and issuances of convective watches. Future

work may be able to develop a model with better skill through the use of a higher resolution model or through stratifying MCS cases into subsets of similar environments.

TABLE OF CONTENTS

LIST OF FIGURES

LIST OF TABLES

ACKNOWLEDGEMENTS

I would like to thank Professor Dr. Roebber for the constant help and mentorship on this research project. I would also like to thank Dr. Clark Evans and Dr. Sergey Kravtsov for the help with coding and ideas with this project. Finally, I would like to thank the UW-Milwaukee atmospheric science department for providing me with teaching assistantship funding.

I. INTRODUCTION

Severe wind producing mesoscale convective systems (MCSs) are common weather phenomena that occur across the United States especially in the warm season. They are beneficial in that they produce generous rainfall which aids the agricultural community but they also are harmful in that they are responsible for considerable damage from severe wind, lightning, and heavy rain. Regardless of negative or positive effects, quality forecasts can improve people's decision making process whether it is to stay safe during these storms or to reduce property damage and agricultural loss.

With these incentives, many in the meteorology community have tried to improve MCS forecasts. These studies included a wide range of research approaches especially in the way that they collected and utilized their data. For example, Jirak and Cotton (2007) gathered environmental meteorological data from NCEP's North American Regional Reanalysis to develop an MCS index that assigns a likelihood of MCS development. Coniglio et al. (2007) used proximity soundings within a 3-hour window of an MCS to develop an updated technique to forecast the short-term motion of MCSs. James et al. (2006) used an idealized model to simulate the conditions of bow echoes to improve the physical understanding of these types of systems. While these studies have made great strides to improve the predictability of these systems, the meteorological community still has insufficient techniques to forecast the track of these systems as suggested by Coniglio et al. (2007).

In this study, an attempt is made to improve forecasts by focusing on the downstream predictability of the path and survival of severe wind producing MCSs that already exist

upstream. The severe wind producing criteria is used because these storms will often produce more damage and create more of a societal impact when compared to MCSs that don't produce severe wind. Furthermore, the requirement that the MCS already exists upstream is to eliminate the development stage where, in most cases, individual thunderstorms coagulate into an organized cluster of storms. This stage is rather complex because the strength and severe capabilities of the storms could be called into question which would affect how these storms progress. Moreover, there may be doubt as to whether the storms will initiate at all since convective initiation remains a difficult forecast challenge (e.g., Banacos et al. 2004) and multiple field studies such as 2002's International H2O Project have been completed to try and expand knowledge on this subject. The exclusion of the development stage is additionally justified because MCSs often travel for very long distances and over many hours. Therefore, many of the areas affected by an MCS will have known the system has already formed and the path and survival of this system become the most critical aspects of the forecast.

Many studies focusing on MCSs have developed evidence that suggests certain variables are important for the maintenance and track of an MCS. Merritt and Fritsch (1984) surveyed the motion of more than 100 MCSs and found that they often track parallel to the contours of the 1000-500hPa thickness. Evans et al. (2001) suggests that when 0-6km mean wind and large-scale forcing are strong, severe surface winds can be supported within derecho (a subset of MCSs) environments. In addition, they note that strong downdrafts, the potential for which are simulated by Downdraft CAPE, can maintain damaging surface winds even when mean winds and large-scale forcing are weak. Coniglio et al. (2007) found that surface-6km shear, 3-8km lapse rates, "best" CAPE, and 3-12km mean wind were the best combination of predictors when forecasting the maintenance of MCSs and they developed the MCS maintenance probability through logistic

regression that was based on these parameters. This study will assess these variables, as well as many more that may help generate a model which is able to improve MCS prediction.

How this study will differ from others is in the method of obtaining data. Some studies used proximity soundings while others used idealized models and manipulated the initial conditions. This study gathers data during the analysis period of the Rapid Update Cycle (RUC) model out ahead of MCSs in the inflow region of the storm. The reason being that the traits of the atmospheric air that are ingested into the system will likely have a great effect on it. Also, since a numerical model is used, the hope is that it keeps the parameters from being affected by the model-produced convection which may skew the data. For example, within the MCS, the model will likely produce much less CAPE since the storm is realizing this energy. A drawback is that the motion of the system is likely dependent on the structure and intensity of the ongoing system itself. For example, the cold pool and rear inflow jet strength will affect the track of MCSs, and this is not directly accounted for in the data. Regardless, a new approach to studying MCSs is attempted in hopes of garnering new methods for predictions.

The goal of this study is to improve the forecast process for MCS events and to improve the understanding of the variables that are most important for the survival and track of these systems. Based on an artificial neural network, a model is developed that uses certain parameters to predict the likelihood that an MCS will move a certain direction. It is hoped that the model produced can improve the decision-making process on issuing convective watches as well as allow businesses to make better financial decisions among other forecast issues. In addition, future studies can use this information to focus on the physics of these systems and continue to advance our understanding.

II. METHODOLOGY

a. Selection of analysis, events, and parameters

To study the environment ahead of an MCS it was determined that a model analysis would provide more data than proximity soundings. Therefore, the 20km Rapid Update Cycle (RUC) model was used since it offers hourly analysis data. To maintain a relatively consistent model configuration and associated biases throughout the study, a 5-year period encompassing the years 2007 to 2011 was chosen. The quality of the model was assessed by Thompson et al. (2003), who showed that the 40km RUC model analysis soundings are a reasonable proxy for observed soundings in supercell environments. They later stated that while the 40km RUC has been replaced by the 20km RUC, SPC forecasters have not identified any undesirable changes and that their study is applicable to the new 20km model. They did note small biases in the model as it tends to be too cool and dry at the surface which, in turn, leads to surface-based CAPE values being lower than proximity soundings. These errors were within typical ranges for radiosonde accuracy so, while there are certain biases in the RUC model, there is evidence to suggest that it can reasonably represent a severe thunderstorm atmosphere.

To develop a dataset of MCSs over this period, base radar reflectivity was combined with surface observations and Storm Prediction Center (SPC) severe storm wind reports to subjectively determine the position of the MCS. For example, if a quasi-linear band of high reflectivity with a width of 100km or greater coincided with multiple severe wind storm reports then the system was determined to be an MCS. If the quasi-linear band of high reflectivity did not coincide with a severe wind storm report, then population density was considered and surface

observations were used to help identify the system. If a system was considered an MCS, the left-most and right-most points of the MCS were gathered at every hour of the MCS's existence. The geographical consideration for these systems was that it had to be in the contiguous United States so the SPC severe storm report archive could be used. In addition, to consider only longer-lived events as Coniglio et al. (2007) did, only systems that lasted five or more hours continuously were included in this study.

This process produced 94 unique events that covered 835 total hours. Figure 1 shows the longevity, in hours, of all the selected cases. Nearly 65% of the cases lasted between 5 and 9 hours while the longest case lasted 19 hours. The dataset included MCSs during the months of April through October, with the most common month being June.

To measure the deviation in the MCS track, two calculations were performed. The first took the midpoint of the MCS at the current hour based on the latitude and longitude of the left-most and right-most points. Then, comparing the midpoint to the midpoint at the previous time step, the angle of the slope was calculated. This angle is in respect to north so an MCS traveling to the east would have an angle slope of 90 degrees. Then, the actual angle of the slope of travel was calculated based on the midpoint of the MCS 3 hours in the future compared to the midpoint at the current time step. Figure 2 shows an example of an MCS that was traveling due east, and deviated 20 degrees to the right of the extrapolated track. Deviations of greater than 90 degrees or less than -90 degrees were excluded since the MCS would no longer be forward propagating. These back-building or training systems accounted for less than 1% of the cases that were originally considered. Other time steps were considered, but 3 hours was selected since lesser time periods would not allow much path deviation, while longer time steps would have severely limited the available data.

Once the selection process was complete, the RUC 20km files from the Research Data Archive website (https://rda.ucar.edu/) were requested and received for each hour of every MCS. MATLAB code was then generated to extract 20 meteorological variables from the analysis time step of these files. Table 1 displays these parameters and their calculations. These parameters were selected in order to assess the conditions necessary for severe storms, in addition to those necessary for MCS longevity. It is widely accepted that instability (i.e. most unstable CAPE), lift, shear (surface to 500 hPa shear), and moisture (850 hPa relative humidity) are essential for severe thunderstorm development. A large majority of the 20 parameters selected were based on this consideration. However, a few parameters were included because they play a critical role in the sustainability of MCSs. The largest equivalent potential temperature difference between the surface and the layers below 600 hPa was selected because it is an indicator of cold pool production, a factor that Evans et al. (2001) claim plays a dominate role in maintaining damaging surface winds with weak large-scale forcing. To account for when large-scale forcing is strong, surface to 500 hPa mean wind speed and direction were selected because Evans et al. (2001) states that with larger mean wind, severe surface winds can occur with relatively weak downdrafts and cold pools.

To determine if any of these parameters can better predict the direction of the path of MCSs, the parameters were collected along a line out ahead of the system. For each case this line was 160 kilometers wide, regardless of the width of the MCS, and consisted of 9 points spaced 20 kilometers apart to coincide with the grid resolution of the model. The line was placed parallel to the line created when connecting the leftmost and rightmost points of the MCS. The midpoint of the line was determined to be 25 kilometers away from the MCS in the direction of motion. To find the direction of motion, the slope of the midpoint of the MCS at the previous

time step to the midpoint of the MCS at the current time was calculated. Each individual point is labeled with a specific number which is consistent among every case, with point 1 (point 9) always on the leftmost (rightmost) side of the MCS's track. An example of this line and the points is shown in Figure 3.

Out of the 835 cases that were gathered, only 454 cases could be used for the analysis. This is because the previous time step was always needed for the calculation of the path of the MCS so the initial time step of every MCS had to be excluded. In addition, the last three hours of an MCS could not be used because of the calculation of the deviation from the MCS's direction of motion. Furthermore, some RUC files contained corrupt data meaning the entire case was excluded.

b. Construction of Models

All of the previously described methods for calculating the variables and deviation of track were completed in MATLAB. This code output excel files which were then input into the software JMP to develop the statistical models. The initial step was to determine if there was a linear relationship that could reasonably predict the track of MCSs. This was done by constructing a (linear) stepwise multiple regression model with the angle of deviation being the dependent variable and the 153 different raw parameters (17)/positions (9) composing the independent variables. To be able to test the quality of the model, a third of the data was randomly held back. When the raw parameter values of the randomly selected data were used, the highest R-squared value that the model produced was never greater than 0.16. This model contained three variables which were surface-500hPa mean wind at point 6, 700hPa temperature

at point 4, and precipitable water at point 8. Since this accounts for only 16% of the variance in the angle of deviation in the development dataset, other methods were then explored. However, it was noted that the stepwise models tested had some variables that were consistently included, such as surface-500hPa mean wind speed, 700hPa temperature, most unstable CAPE, and precipitable water.

The next approach that was taken was to standardize the parameters by its along-line mean for each case. This was done by calculating the mean of all 9 points along the line for each parameter and case and then subtracting the actual value by the mean to get the anomaly. The reason for this was that the gradient of the parameters may play a bigger role than the actual value of the parameter. In other words, a certain case may have had most unstable CAPE ranging from 1000 j/kg to 3000 j/kg while another may have had uniform most unstable CAPE of 4000 j/kg. In the first case, the MCS may have progressed into the region of higher most unstable CAPE while in the second case the system may have evolved based on other parameters. When a similar linear stepwise model was constructed, five parameters proved to be the best predictors including the precipitable water at point 8, most unstable CAPE at point 5, 700hPa temperature at point 4, surface-500hPa mean wind at point 6, equivalent potential temperature difference at point 2, and 700-500hPa lapse rate at point 4. These parameters again only explained a small amount of the variance since the R-squared value was only 0.14.

Since the linear stepwise models proved to be rather poor, a different approach was taken which was to separate the angle deviations of the MCSs into three classes. The reason for this approach was that the predictors may not be able to accurately predict the angle of deviation but they may be able to predict when a certain case may be susceptible to deviating to the right, left or staying on the current path. These classes are based on standard deviations from the mean.

Since the distribution of the angle of deviation has rather high kurtosis, a small standard deviation of 0.5 was used to make relatively even classes. The three classes consisted of "Left", "Middle", and "Right". The "Left" class had angles of deviation less than -7.69 degrees, the "Right" class having angles of deviation of greater than 7.01 degrees, and the "Middle" class having angles of deviation between less than 7.01 but greater than -7.69 degrees. The amount of cases in each of these classes were 117 to the "Left", 243 in the "Middle", and 94 to the "Right". To account for the uneven amount of "Middle" cases, 50% were excluded by randomly selecting "Middle" cases with a random number generator. This produced 108 "Middle" cases that were then used in the model. The usefulness of the 0.5 standard deviation was also considered because it should make sense meteorologically. A deviation of about 7 degrees over a three-hour period would mean that an MCS would deviate roughly 22 kilometers if it was assumed that the MCS had a forward propagation speed of 60 km per hour. A deviation of this length was considered large enough to proceed with the stratification of classes. Nonetheless, the best (linear) stepwise multiple regression model for this approach did not yield a model that improved upon the R-squared of 0.16 found in other approaches.

With stepwise multiple regression models explaining such a small amount of the variance, an artificial neural network was built to predict the track of the MCSs. Given that linear methods were unsuccessful in predicting the path, non-linearities may exist in the data which an artificial neural network might capture. To predict which class the MCS would take, the artificial neural network produced a probability for each system to track down each class and the class that had the highest probability was used for the model's prediction. Just as in the linear models, one third of the data was held back such that the model can be tested. Numerous combinations of variables and nodes were attempted to produce the best model. For example, for each new set of

variables that were tested, the neural network was run with numerous different nodes in an attempt to capture the non-linearities in the data. Then, different variable combinations, such as taking the middle point of certain variables and switching up the number of variables, were tested with different nodes and so on. The combination of variables that proved to be most beneficial in predicting the track of MCSs was the precipitable water at point 8, most unstable CAPE at point 5, 700hPa temperature at point 4, surface-500hPa mean wind at point 6, 700-500hPa lapse rate at point 4, and equivalent potential temperature difference at point 2. Prior to analysis, a check for collinearity was performed between variables and within a variable for a given position along the line. None of the variables needed to be excluded based upon these tests.

III. RESULTS

The results from the artificial neural network, described in the methodology section, are analyzed here. All calculations and equations used to construct this model can be found in the appendix. Figure 4 shows a schematic diagram from Roebber et al. (2003) that depicts the structure of the neural network. This model has 6 inputs (i.e., D=6) which were described in the methodology, 21 hidden nodes (K=21), and 3 outputs (M=3) consisting of the three possible track deviations. The hidden nodes use an equation with a hyperbolic tangent to connect the 6 input variables with the 3 output classes. The reason 21 hidden nodes were chosen was that it produced the most stable model. In other words, having 21 hidden nodes allowed the model to consistently predict the correct classes despite the different randomly selected cases that were included in each run of the model.

Table 2 shows the contingency table associated with the neural model that produced the best prediction of the track. Table 3 shows that the model percent correct is 46.5%, Heidke skill score 0.156, and a threat score 0.303. Although these statistics demonstrate relatively small skill, these compare favorably, for example, to those for NOAA's Weather Prediction Center's Day 1 forecasts for heavy rainfall in the warm season (http://www.wpc.ncep.noaa.gov/images/hpcvrf/d110.gif).

The question becomes how can a forecaster successfully implement this information into their forecast process? Evaluating the predictions for each class and considering every one of the 454 cases revealed that the model's "Left" ("Middle", "Right") forecasts had a probability of detection of 0.55 (0.46, 0.36) while the false alarm rates for the "Left" ("Middle", "Right")

forecasts were 0.64 (0.41, 0.57). To examine the model's biases, the threat score and bias were calculated for each class. The "Left" ("Middle", "Right") forecasts had a threat score of 0.28 (0.35, 0.24) and a bias of 1.56 (0.79, 0.85). The threat scores for an equal-frequency random forecast based on the climatology of each class produced 95th percentiles of 0.147-0.150 (0.363-0.367, 0.116-0.123) for the "Left" ("Middle", "Right") classes. When considering this, the model proved to be skillful when predicting "Left" and "Right" classes because it's threat scores were outside of the 95th percentiles of 1000 randomly produced forecasts. In addition, the model was not skillful when predicting "Middle" cases since the threat score was less than the 95th percentiles. These numbers also indicate that the model has a "Left" bias, meaning that there were more "Left" forecasts than actual events. The model underpredicts "Middle" and "Right" cases and, to a lesser extent, it overpredicts the "Left" cases. This is likely due to the fact that when the cases were selected for training, despite efforts to balance numbers on each category, there were still more "Left" cases than in the two other classes.

To make sure the model is not fitting to the noise, the analysis is broken down into performance stratified by both the training dataset and the validation dataset (Tables 4 and 6). Neither dataset includes the 135 "Middle" cases that were excluded to develop relatively even track change categories. From the 319 remaining cases, the training dataset was gathered by randomly selecting two-thirds of the cases and the validation dataset consists of the remaining one-third. In both cases, the percent correct (Training: 46.7% and Validation: 48.6%) and the Heidke skill score (Training: 0.19 and Validation: 0.21) were higher than when the model was used on all of the cases (Seen in Tables 5 and 7). One possible reason that these numbers are higher than the model for all of the cases is that when all cases are considered, only "Middle" cases are added back in. The "Middle" cases did not have the best threat scores and bias in the

training dataset so it likely decreased the skill of the model adding those back in. To assess the skill and biases of the model, threat scores and biases were calculated for each of the three tracks. For the training dataset, the "Left" ("Middle", "Right") forecasts had a threat score of 0.36 (0.27, 0.28) and a bias of 1.09 (1.27, 0.61). This analysis deviates from the analysis for all of the cases because the model's skill is best when forecasting "Left" cases while the slight overprediction bias is much smaller than for all of the cases. The model predicts the "Right" cases with better skill but it has a significant underprediction of these events. Where the model performs worse, is the "Middle" cases because the threat score drops nearly 0.08 when compared to all cases and it switches to an overprediction bias. The validation dataset is very similar to the training dataset as the "Left" ("Middle", "Right") forecasts had a threat score of 0.35 (0.3, 0.3) and a bias of 1.1 (1.11, 0.71). In fact, the threat scores increase while the bias decreases for the "Middle" and "Right" cases. The increased threat scores and decreased bias likely is a result of the relatively even cases in each of the three track change classes.

Next, a sensitivity analysis was performed on each variable to determine its significance within the model. The first method attempted for sensitivity analysis was to fit the six (independent) variables within the neural network into a (linear) stepwise multivariate regression model with the neural network model's probability of a certain track change as the dependent variable. For each of the three different track changes, four variables were statistically significant as they had a p-value of less than 0.01. The only variable to be statistically significant for each track change was surface-500hPa mean wind. Conversely, there were no variables that were not at least once statistically significant.

Figures (5 through 7) show the four statistically significant variables for each of the three possible track changes. For the "Left" cases, the variable that appears to have the best correlation

is surface-500hPa mean wind. The stronger the surface-500hPa mean wind, the more likely the model is to predict that the system will track to the “Left”. The rest of the variables do not seem to have any correlation except for a possible slight correlation between higher equivalent potential temperature difference and a better probability to track “Left”.

For the “Middle” cases, there appears to be weak correlations between the variables and the probabilities. The only case you can make is the surface-500hPa mean wind has a slight correlation between weaker winds and having a higher chance of tracking in the “Middle”. For the “Right” cases, correlation seems present in surface-500hPa mean wind in which it shows that weaker wind leads to the model predicting a better chance that the system will move to the “Right”. There may also be weak correlation between lower values of equivalent potential temperature difference (higher values of most unstable CAPE) and a higher chance of a “Right” track.

Based on these correlations, a slightly different sensitivity analysis was performed to further investigate their ability to predict the track of an MCS. The median of each of the 6 parameters was chosen as a baseline for this analysis. To test the sensitivity of 4 of the correlated variables, their values were modified one by one. For example, to test the sensitivity of the model with respect to surface-500hPa mean wind, arbitrary surface-500hPa mean wind values were inputted instead of the median value while the rest of the parameters were held constant. The model then calculated the probabilities of each class based on the new surface-500hPa mean wind value. Figure 8 shows the results from this analysis for the variables, surface-500hPa mean wind, most unstable CAPE, equivalent potential temperature difference, and precipitable water. For surface-500hPa mean wind, this reinforces the previous conclusions that smaller (higher) values give a greater chance for MCSs to track in the “Middle” and “Right” (“Left”).

Furthermore, higher values of equivalent potential temperature difference (precipitable water) give a greater chance for MCSs to track to the "Left" ("Middle") while lower values give a greater chance for MCSs to track to the "Right" ("Right"). For most unstable CAPE, there were no correlations between higher or lower values and greater probabilities of a certain track.

When examining parameters individually, surface-500hPa mean wind stands out as the parameter that shows the largest difference between the inner quartile range in the three categories. Figure 9 shows cases that had weaker mean wind were more likely to move to the right than cases that had relatively stronger mean wind. The other parameters did not show any clear differences between the inner quartile ranges of the three possible movements.

Once this analysis was completed, an attempt was made to add other variables to improve the artificial neural network. 1000-500hPa thickness was added along with surface-500hPa mean wind direction. Unfortunately, these parameters were unsuccessful in improving the artificial neural network. Since multiple papers, such as Merritt and Fritsch (1984), have found that MCSs typically follow thickness gradients, the 1000-500hPa thickness was stratified into three sections to account for the gradient. The thickness at point 1 (4,7) was subtracted by the thickness at point 3 (6,9) to develop a gradient in the path of the MCS. This new parameter was also ineffective in improving the model.

A. Case study

Three case studies, one for each track change, were evaluated to assess the usefulness of the model. The "Right" mover case occurred on June 23, 2009 as an MCS developed over northwest Iowa and Southwest Minnesota and began tracking eastward (Figure 10). Over the

next 6 hours the MCS began to deviate to the right and finally began to weaken in extreme southeastern Iowa. Table 8 shows that the model correctly predicted the MCS to have a track change to the "Right" for 4 hours. The below average surface-500hPa mean wind is likely the biggest reason as to why it deviated to the right since all hours had negative values of mean wind. Figure 11 shows the mesoanalysis archive 850-300hPa mean winds at 18 UTC which were very light. An application of the model in this case would be to consider these light mean winds and realize that the system likely has a much higher chance of deviating to the right than other MCSs. The other parameter that may give some insight into why the MCS tracked to the "Right" is the equivalent potential temperature difference which was near zero or below zero in many of the hours. This may indicate that the system had limited cold pool potential and that other factors like CAPE may have played a bigger role in determining the track of the system.

The second case occurred on June 12, 2009 as an MCS developed over south-central Kansas heading east-southeastward. Surface-500hPa mean winds in this case were near zero for nearly every hour which was a factor in the model correctly predicting that the MCS would track in the "Middle" path (Figure 12). The 850-300hPa mean wind seen in Figure 13 shows that this system had an environment with moderate mean winds which helped it maintain the path it was on. Since lower values of the surface-500hPa mean wind make a track to the "Middle" and the "Right" more likely, other variables are needed to determine the track change (Table 9). In this case, the equivalent potential temperature difference being positive and near 5 means that it is associated with lower probabilities on tracking "Right". The other 4 parameters had values near zero as well meaning there was no strong indication that this system would deviate "Right" or "Left".

The last case occurred on April 26, 2011 as an MCS developed over southwestern Arkansas moving northeastward. This system tracked to the "Left" due in large part to the relatively strong mean wind (Figure 14). The surface-500hPa mean wind values for each hour of the case were 0.3 and 0.5 m/s which falls in the area of enhanced probabilities for the system to track "Left" (Table 10). Figure 15 shows that the 850-300hPa mean wind was much stronger in the this case than the other two.

The sensitivity analysis and the case studies reveal that the strength of the surface-500hPa mean wind can help delineate between whether a case will track "Left" and when it will track to the "Middle" or "Right". One possible physical reason for this is that the cases with stronger surface-500hPa mean wind may be identified as a system similar to a serial derecho as described in Johns and Hirt (1987). These systems typically are associated with an extended squall line with line-echo wave patterns and a well-defined, migratory low pressure system, hence the better likelihood for stronger surface-500hPa mean winds. When the surface-500hPa mean wind is weaker, the MCSs may be similar to progressive type derechos as explained by Johns and Hirt (1987). These systems typically have one bow echo and form along a stationary front in a stagnant upper level pattern.

Perhaps the most difficult decision that forecasters using these results would have, would be to determine between a "Middle" and "Right" track change. This is because the lower the surface-500hPa mean wind, the more likely the MCS is to travel to the "Middle" and the "Right". In these cases where the surface-500hPa mean wind is light, it is best to look at a combination of parameters because one parameter does not stand out above the rest. The sensitivity analysis revealed that lower equivalent potential temperature differences at point 2 increase (decrease) the chance for a system to track "Right" ("Middle"). In addition, precipitable

water values at point 8 greater than 5 (less than -5) increases the probability that the system tracks in the “Middle” (“Right”). Errors when using this forecast model to predict a “Middle” case versus a “Right” case do not always fall in the “Middle” or “Right”. In other words, while errors when predicting “Right” cases often end up with the highest probability being in the “Middle” class (38) versus “Left” cases (8), more errors end up in the “Left” class (44) than the “Right” class (35) when predicting the “Middle” class.”

IV. CONCLUSIONS AND DISCUSSION

This study looked at RUC analysis parameters from the years 2007 to 2011 in an attempt to improve the forecasting process for MCS track changes. Since (linear) stepwise multiple regression models were unsuccessful in developing a useful model, an artificial neural network model was developed. This model incorporated the parameters, precipitable water at point 8, most unstable CAPE at point 5, 700hPa temperature at point 4, surface-500hPa mean wind at point 6, equivalent potential temperature difference at point 2, and 700-500hPa lapse rate at point 4. This model had a threat score of 0.30 and a Heidke skill score of 0.156 which demonstrates relatively small skill but compares favorably to other warm season forecasts. When considering each of the three classes, the model had the best threat score when predicting the "Middle" cases and the worst threat score when predicting "Right" cases. In addition, it had a considerable overforecasting bias for "Left" cases and a underforecasting bias for "Middle" and "Right" cases.

Perhaps the most useful product of this study was showing the importance of the surface-500hPa mean wind on predicting the change in track of MCSs. In cases where the surface-500hPa mean wind at point 6 is higher than zero, there is a better chance for MCSs to track "Left" and the chances increase with higher surface-500hPa mean winds values. Surface-500hPa mean wind below zero increases the probability that the MCS will track to the "Middle" or "Right".

Other parameters performed relatively poorly during the sensitivity analysis. The only other parameters that indicated they were useful in predicting the track of an MCS were equivalent potential temperature difference and most unstable CAPE. Lower values of equivalent

potential temperature difference and higher values of most unstable CAPE were weakly correlated with a higher chance of a “Right” track.

It is important to note that this method for predicting the track of MCSs is limited in that it is only looking out ahead of the systems. The environment within and behind the MCS plays a large role in the evolution of the system. Therefore, any model developed based on the parameters out ahead of an MCS cannot be the only product considered when forecasting its track. Nonetheless, this study proved that a skillful model can be developed based solely on the meteorological parameters ahead of an MCS. Other limitations include the possibility that the environment may change within the 3 hours that is required to determine the track change. Environments can change drastically within a matter of an hour and this can influence the track of the system which would not be captured within the model in this study.

The results from this study also indicate that there is a need for future work to enhance the forecast process on this problem. Future studies can use a newer, higher resolution numerical model, like the Rapid Refresh model, to assess the atmosphere better than the RUC 20km used in this study. It also may be worthwhile to stratify cases into different types of MCS environments. For example, cases can be stratified into the two types of environments that Johns and Hirt (1987) documented for derechos (a subset of MCSs): serial derecho environments which have relatively strong forcing with the derecho developing ahead of a cold front; and progressive derecho environments which have relatively weak forcing and derechos developing along stationary fronts.

Other parameters or calculations could be used to further improve the model. For example, different levels of mean wind can be used than the surface-500hPa column used in this study. Downdraft CAPE could be considered along with other composite parameters like the

probability of MCS maintenance or the energy-helicity index. Finally, arbitrarily selected aspects of this study could be reconsidered like the 3-hour time step to determine the track change in an MCS and the 25km distance from the leading edge of the MCS to the line where the meteorological parameters were collected. A useful study may be to consider longer-lived MCSs, like derechos, and to lengthen the time step for determining the track change. This might improve the track changes for higher impact events that represent a substantial forecast challenge.

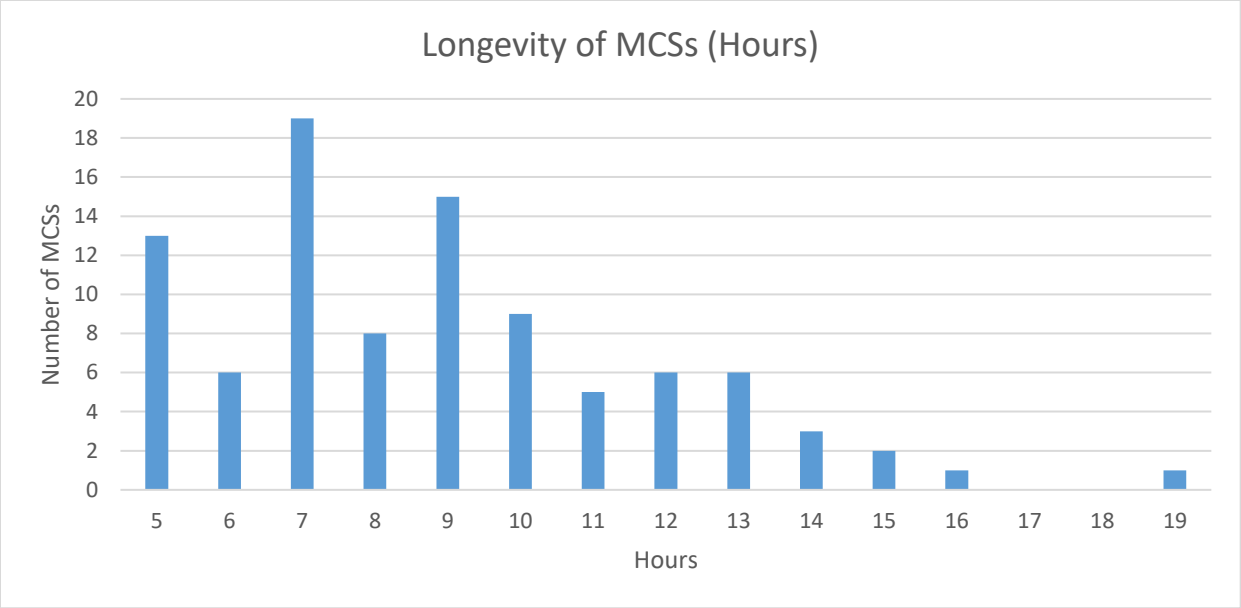

Figure 1. Histogram of the longevity in hours of each MCS event.

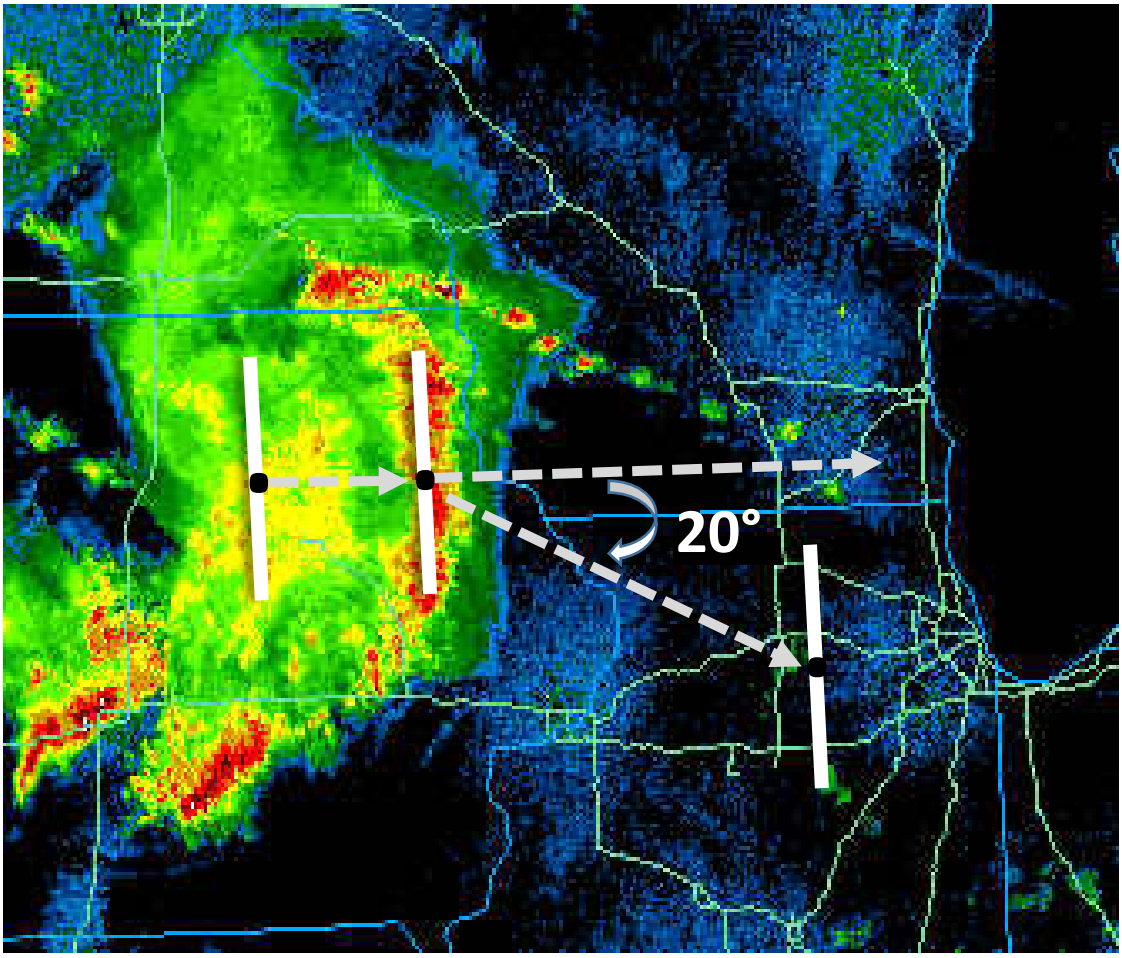

Figure 2. An MCS deviating 20 degrees to the right of the original track.

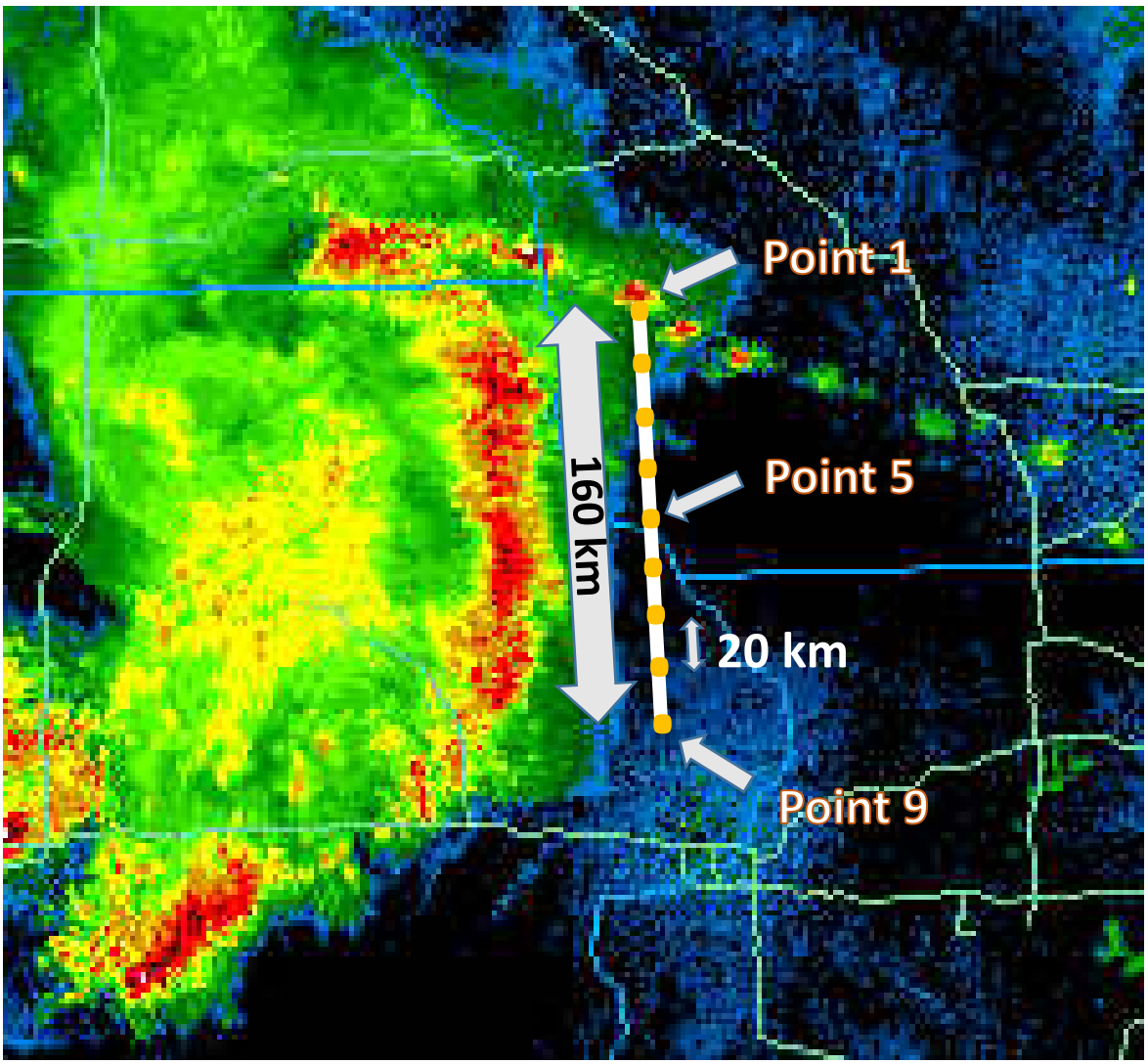

Figure 3. A depiction of the line in which that RUC model data is gathered from. Point 1 is the leftmost point, point 9 is the rightmost point. There is 20km between each point and the length of the line is 160km.

Parameter	Calculation	Units
Low-level Equivalent Potential Temperature (Θ_e) Difference	Surface Θ_e – minimum Θ_e in atmosphere at 600hPa and below	K
850hPa Wind Direction with respect to MCS motion	850hPa wind direction – MCS direction	Degrees
700-500hPa Lapse Rate	700hPa temperature – 500hPa temperature	C
Sfc-500hPa Mean Wind Speed	Finding the sum of the u and v components from sfc to 500hPa and calculating their magnitude	M/S
300hPa Wind Speed	Model output	M/S
850hPa Wind Speed	Model output	M/S
Most unstable CAPE	Model output	J/KG
Surface based CAPE	Model output	J/KG
Most unstable CIN	Model output	J/KG
Surface based CIN	Model output	J/KG
Boundary Layer Storm Relative Helicity	Model output	M^2/S^2
Precipitable Water	Model output	Kg/M^2
Surface-500hPa Wind Shear Speed	Finding the magnitude of the winds after taking the difference between the sfc and 500hPa u and v components.	M/S
700hPa Temperature	Model output	C
850hPa Temperature	Model output	C
700hPa Relative Humidity	Model output	%
850hPa Relative Humidity	Model output	%
Sfc-500hPa Mean Wind Direction with respect to MCS motion	Surface-500hPa mean wind direction – MCS direction	Degrees
1000-500hPa Thickness	1000hPa height - 500hPa height	M
1000-500hPa Thickness Gradient	Thickness at point 3 (6,9) – thickness at point 1 (4,7)	M

Table 1. The 20 meteorological parameters that were included in this study, their calculations, and their units are displayed in the three columns of the table.

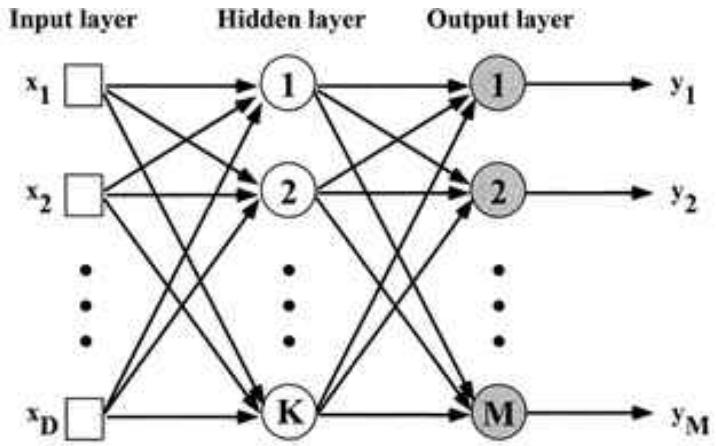

Figure 4. Schematic diagram of a neural network model from Roebber et al. (2003). This model has single-hidden-layer with D (6) inputs, K (21) hidden layer processing elements and M (3) outputs.

		Predicted Class			
		Left	Middle	Right	Total
Actual Class	Left	65	44	8	117
	Middle	93	112	38	243
	Right	25	35	34	94
	Total	183	191	80	454

Table 2. Contingency table of the artificial neural network model for all cases.

All Cases			
Heidke Skill Score	0.15637904		
Threat Score	0.30272597		
Percent Correct	46.4757709		
	Left	**Middle**	**Right**
Probability of Detection	0.55555556	0.46090535	0.36170213
False Alarm Rate	0.64480874	0.41361257	0.575
Threat Score	0.27659574	0.34782609	0.24285714
Bias	1.56410256	0.78600823	0.85106383

Table 3. List of different skill scores and statistical analyses for all cases.

		Predicted Class			
Actual Class		Left	Middle	Right	Total
	Left	43	29	5	77
	Middle	25	34	12	71
	Right	16	27	23	66
	Total	84	90	40	214

Table 4. Contingency table of the artificial neural network model for the training dataset.

All Cases			
Heidke Skill Score	0.19479834		
Threat Score	0.30487805		
Percent Correct	46.728972		
	Left	**Middle**	**Right**
Probability of Detection	0.55844156	0.47887324	0.34848485
False Alarm Rate	0.48809524	0.62222222	0.425
Threat Score	0.36440678	0.26771654	0.27710843
Bias	1.09090909	1.26760563	0.60606061

Table 5. List of different skill scores and statistical analyses for the training dataset.

		Predicted Class			
Actual Class		Left	Middle	Right	Total
	Left	22	15	3	40
	Middle	13	18	6	37
	Right	9	8	11	28
	Total	44	41	20	105

Table 6. Contingency table of the artificial neural network model for the validation dataset.

All Cases			
Heidke Skill Score	0.21118531		
Threat Score	0.32075472		
Percent Correct	48.5714286		
	Left	**Middle**	**Right**
Probability of Detection	0.55	0.48648649	0.39285714
False Alarm Rate	0.5	0.56097561	0.45
Threat Score	0.35483871	0.3	0.2972973
Bias	1.1	1.10810811	0.71428571

Table 7. List of different skill scores and statistical analyses for the validation dataset.

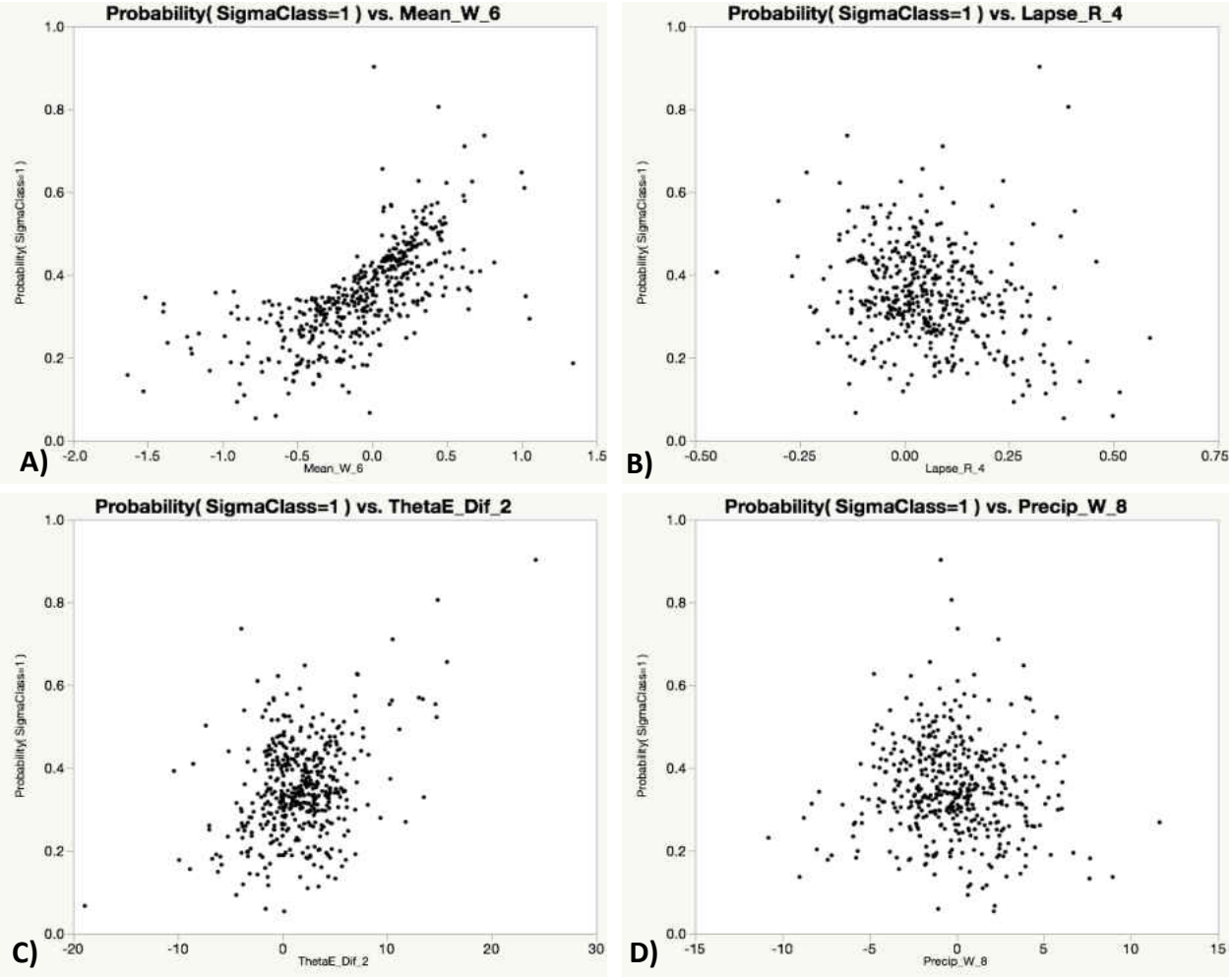

Figure 5. (a)-(d) Scatter plots with the dependent variable on the y axis indicating the probability for an MCS to track "Left" and the independent variable (a) surface-500hPa mean wind, (b) 700-500hPa lapse rates, (c) equivalent potential temperature difference, and (d) precipitable water.

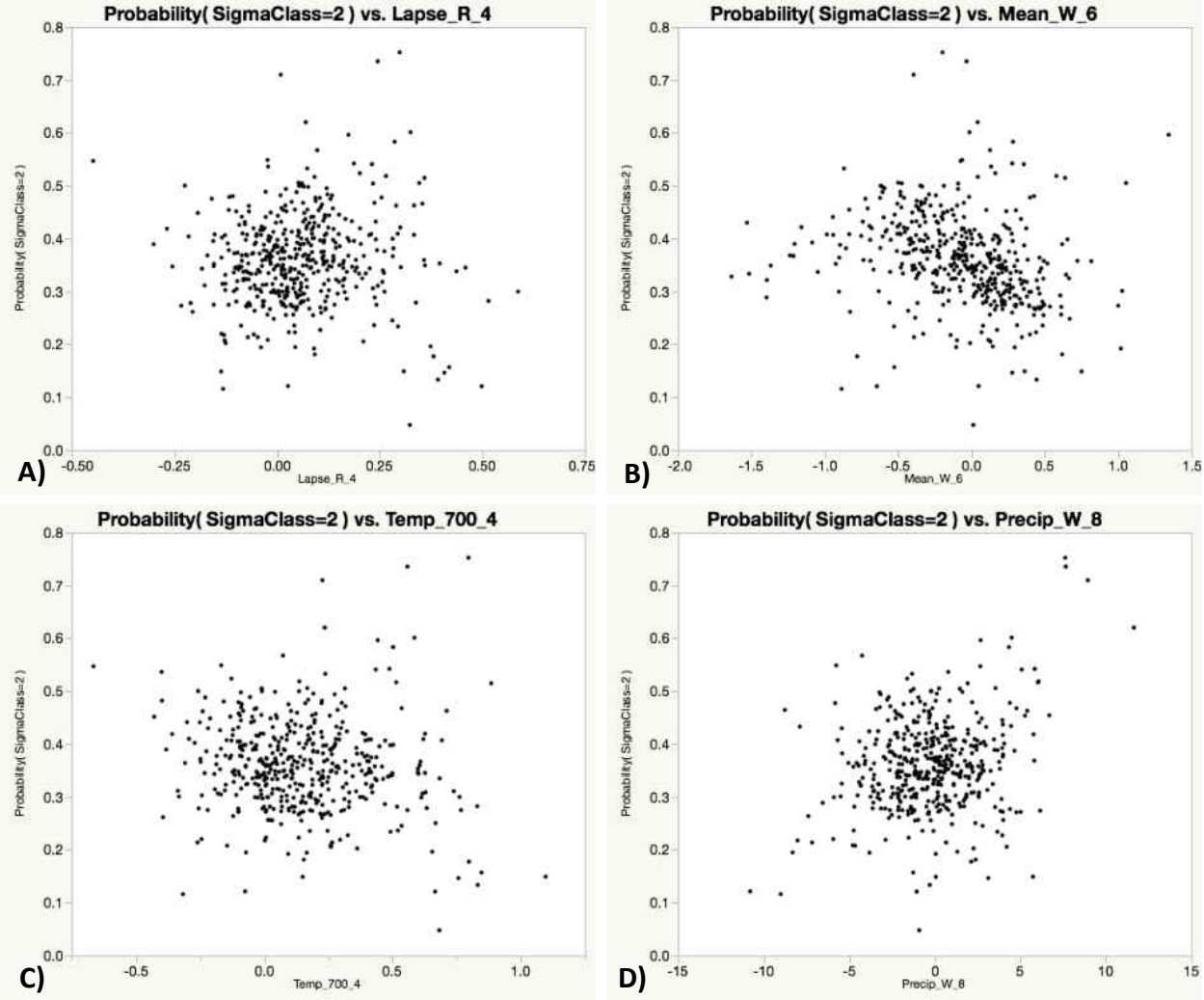

Figure 6. (a)-(d) Scatter plots with the dependent variable on the y axis indicating the probability for an MCS to track "Middle" and the independent variable (a) 700-500hPa lapse rates, (b) surface-500hPa mean wind, (c) 700hPa temperature, and (d) precipitable water.

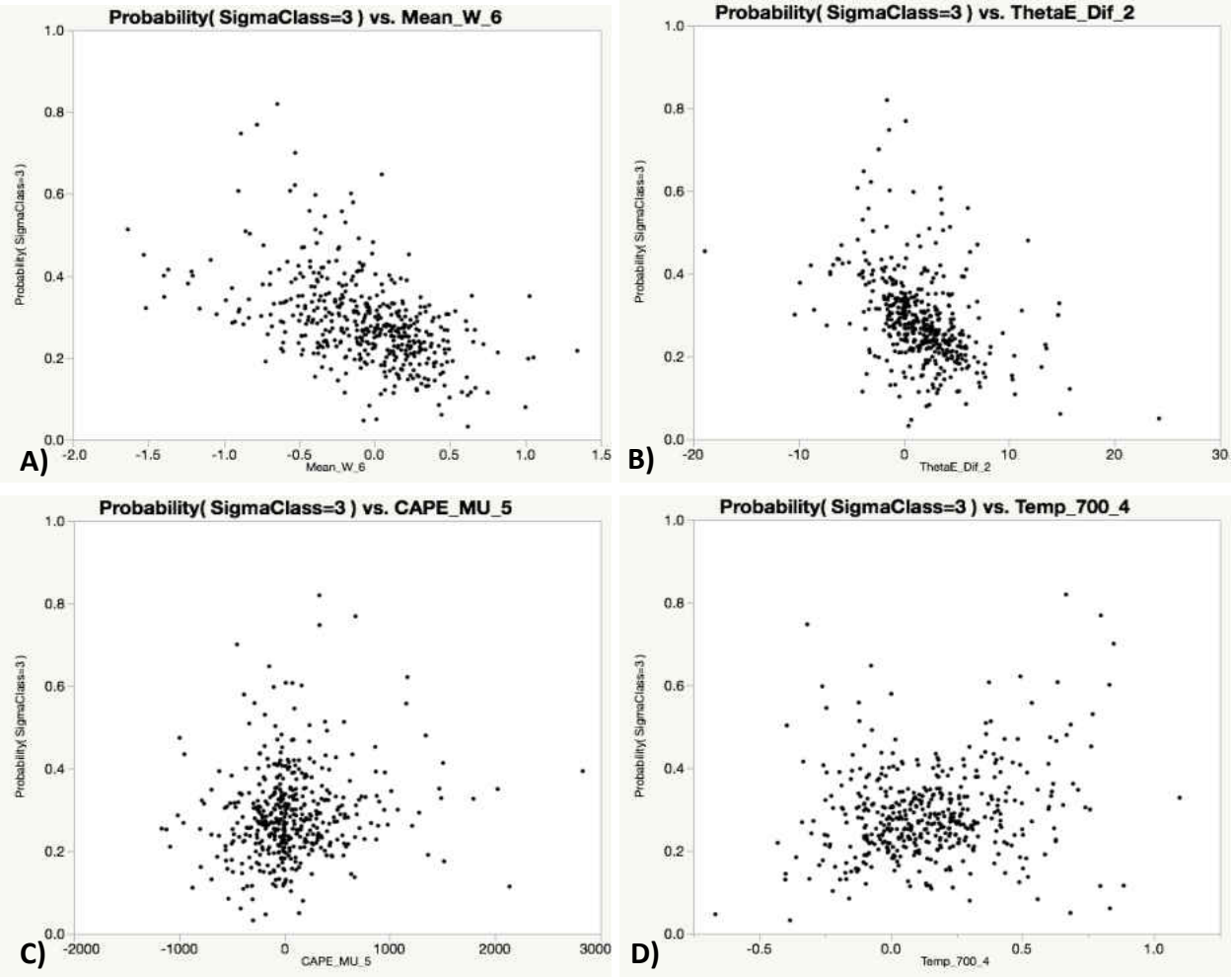

Figure 7. Scatter plots with the dependent variable on the y axis indicating the probability for an MCS to track "Middle" and the independent variable (a) surface-500hPa mean wind, (b) equivalent potential temperature, (c) most unstable CAPE, (d) 700hPa temperature.

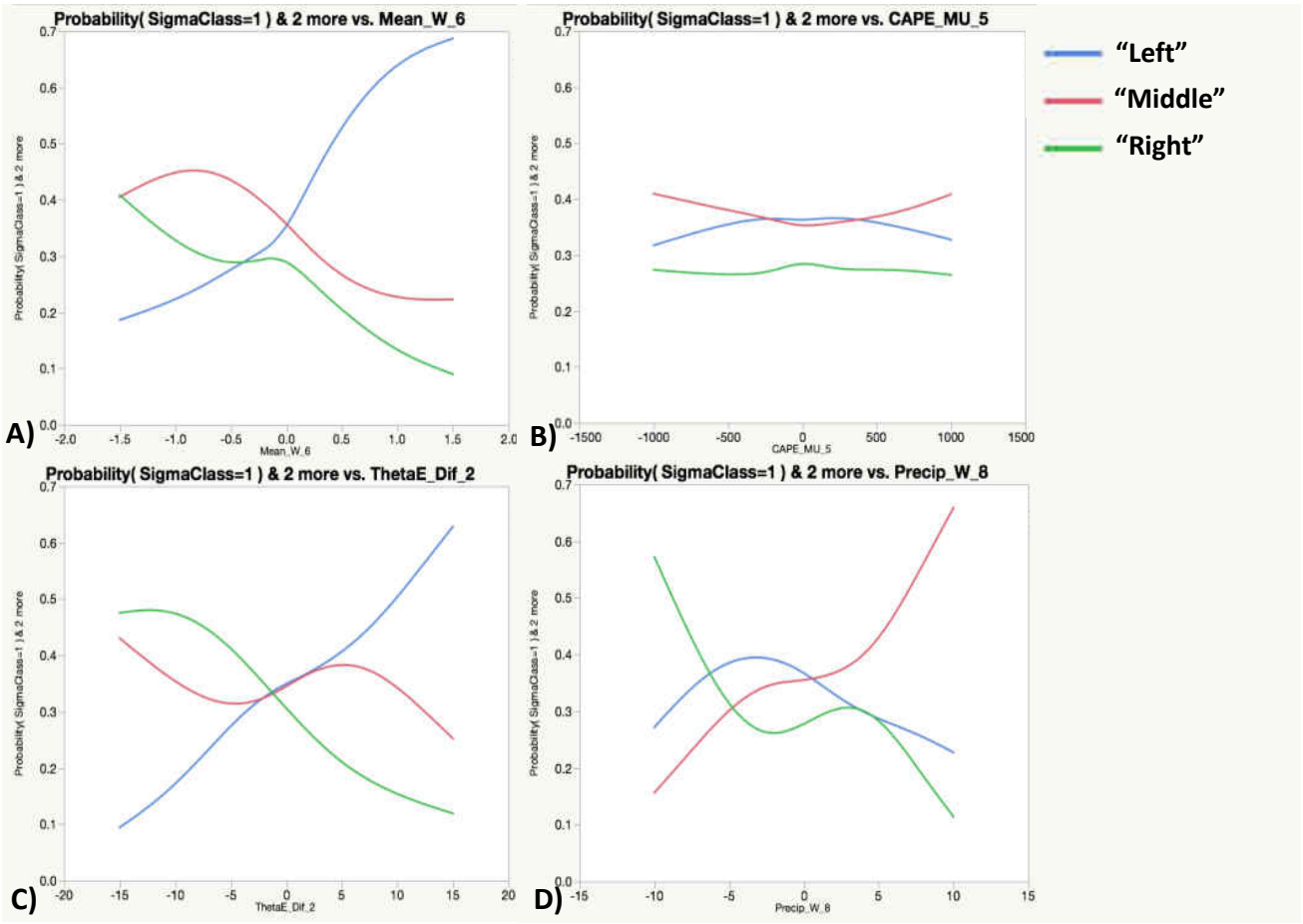

Figure 8. (a)-(d) Plots with the dependent variable on the y axis indicating the probability for an MCS to track "Left" in blue, "Middle" in red, and "Right" in green, and the independent variable (a) surface-500hPa mean wind, (b) most unstable CAPE, (c) equivalent potential temperature, (d) precipitable water.

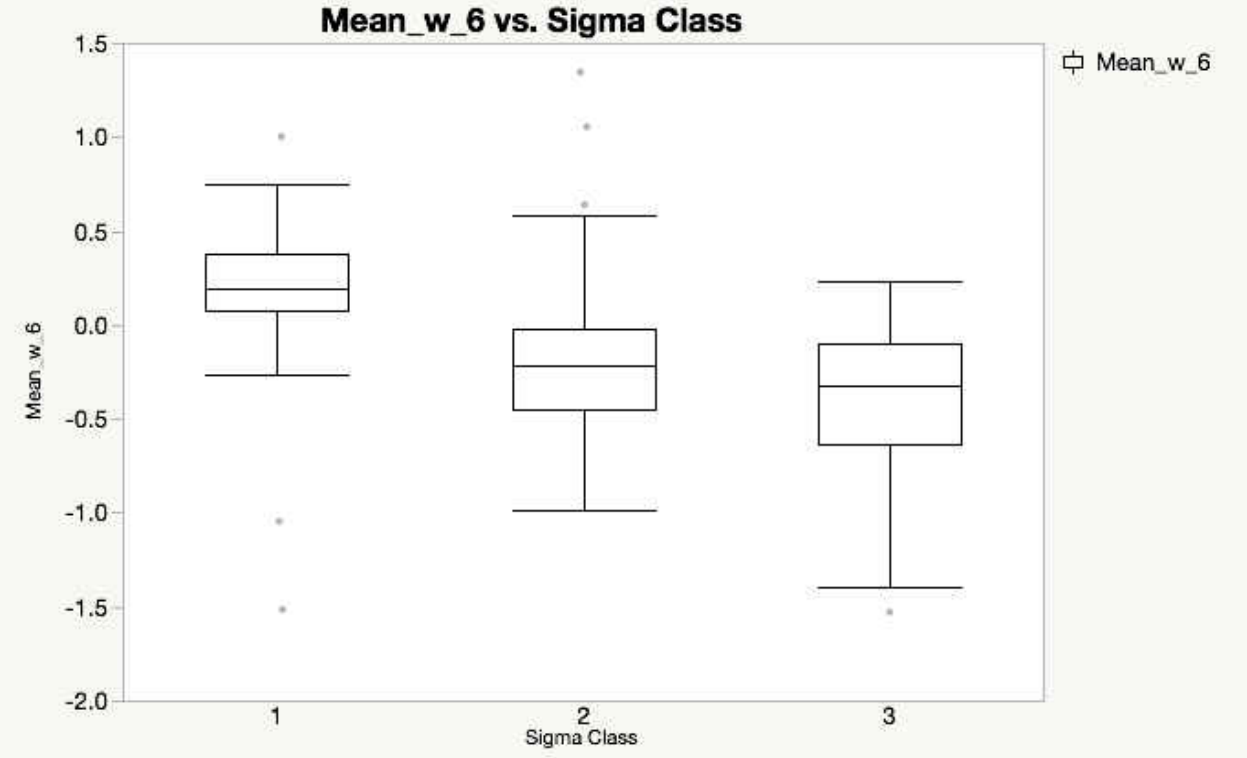

Figure 9. Box plot with the surface-500hPa mean wind as the dependent variable and the "Left" (1), "Middle" (2), and "Right" (3) as the independent variables.

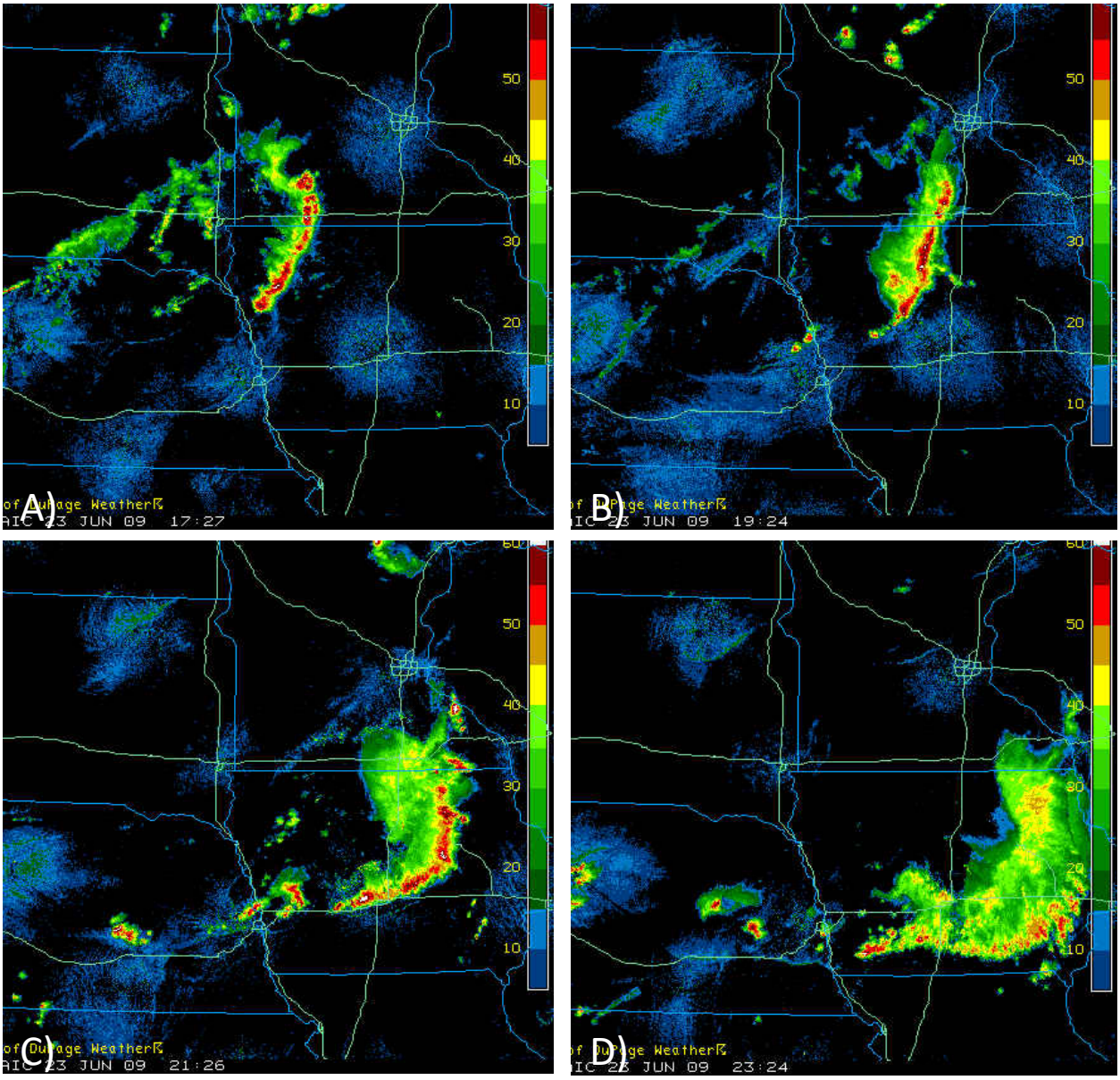

Figure 10. (a)-(d) Base reflectivity for the June 23, 2009 MCS at (a) 17 UTC, (b) 19 UTC, (c) 21 UTC, (d) 23 UTC. These were gathered from http://www2.mmm.ucar.edu/imagearchive/.

Time (UTC)	Actual Class	Degree of Deviation	700hPa Temp	Precip Water	MU CAPE	Sfc-500hPa Mean Wind	700-500hPa Lapse Rates	Theta-e Dif	Forecast Class	Hit
00Z	1	-18.52	-0.22	-2.62	62.08	0.5	-0.15	-0.42	1	1
01Z	1	-24.57	0.25	-0.72	-6.95	0.5	0.04	0.26	1	1
02Z	2	1.73	0.15	0.22	-499.22	0.4	-0.03	1.89	1	0
03Z	2	-2.14	0.4	3.9	436.8	0.46	0.07	5.7	1	0
04Z	1	-10.21	0.47	0.25	549.9	0.33	0.17	4.54	1	1

Table 8. The 6 meteorological parameters that were included in the neural network, in addition to, the actual and forecast class, the angle of deviation, and hits for the June 23, 2009 MCS. A hit of 1 indicates the actual and forecast track were identical while a 0 means they were different.

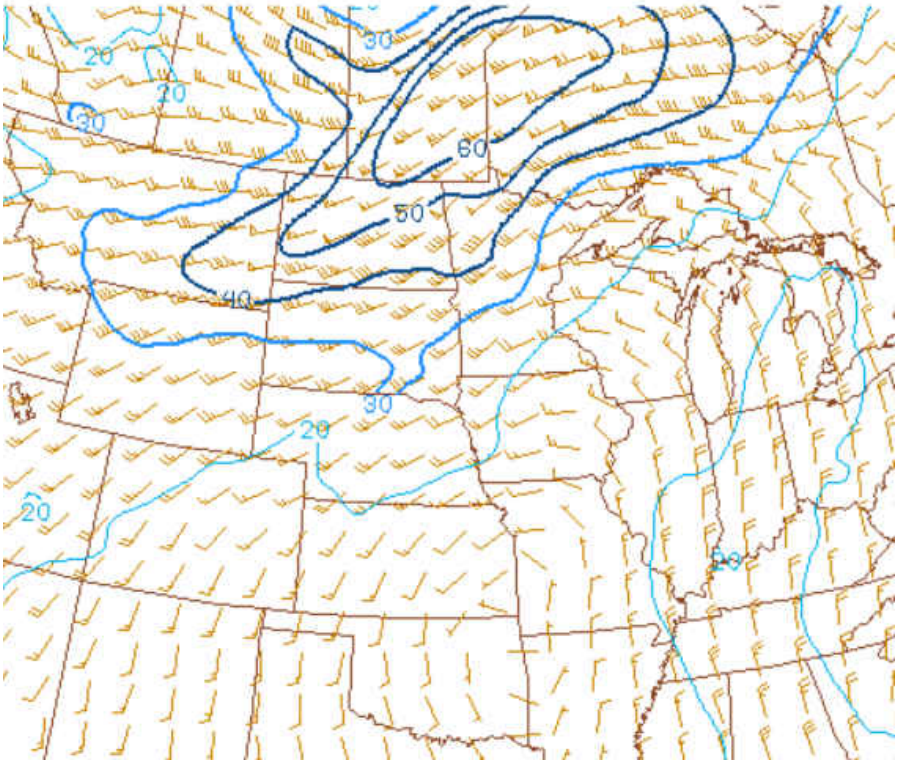

Figure 11. June 23, 2009 850-300hPa mean wind at 18 UTC.

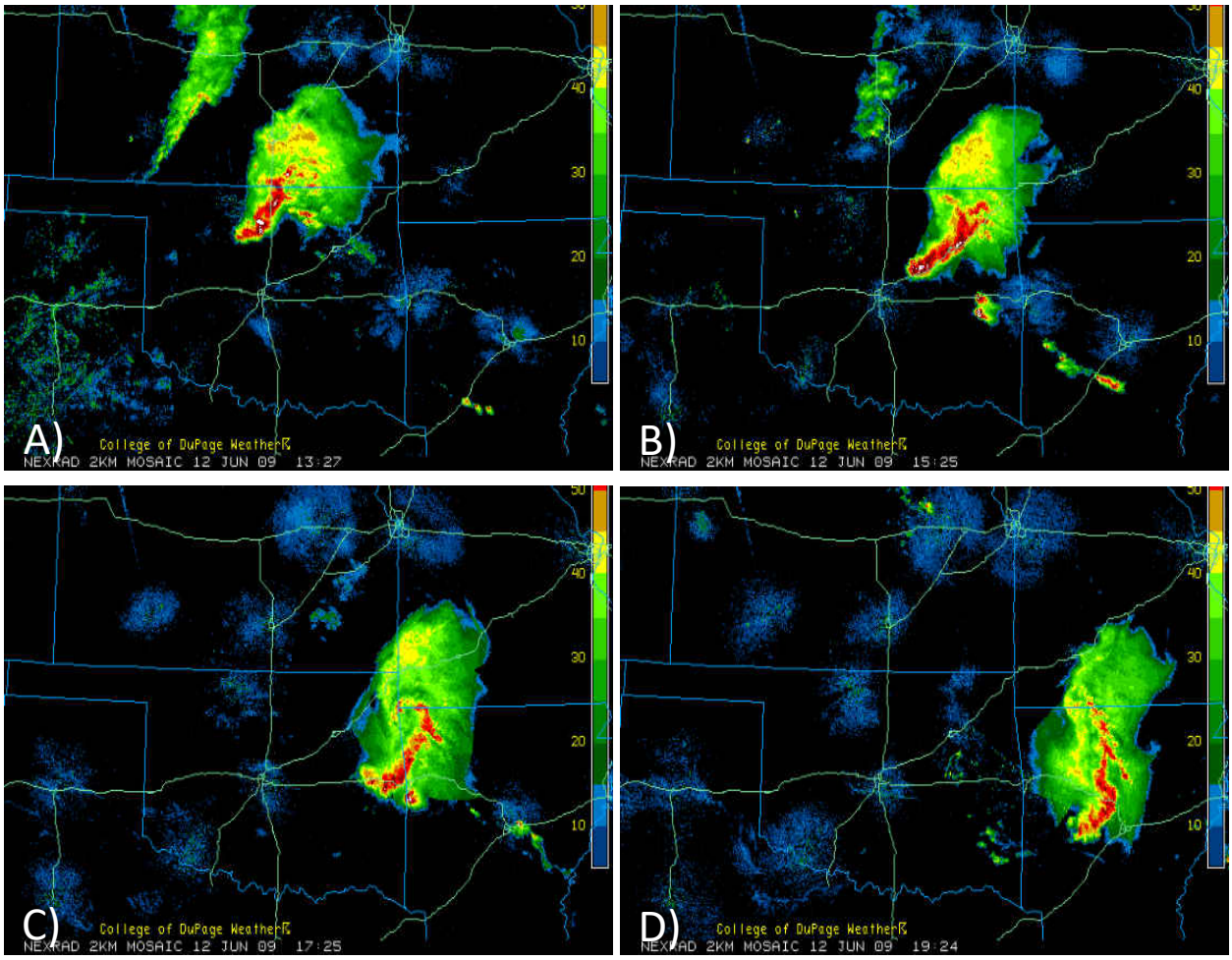

Figure 12. (a)-(d) Base reflectivity for the June 12, 2009 MCS at (a) 13 UTC, (b) 15 UTC, (c) 17 UTC, (d) 19 UTC. These were gathered from http://www2.mmm.ucar.edu/imagearchive/.

Time (UTC)	Actual Class	Degree of Deviation	700hPa Temp	Precip Water	MU CAPE	Sfc-500hPa Mean Wind	700-500hPa Lapse Rates	Theta-e Dif	Forecast Class	Hit
13Z	2	2.95	-0.01	-1.23	-270.98	-0.09	0.23	2.7	2	1
14Z	2	-2.91	0.1	-2.32	498.64	-0.28	0.29	4.72	2	1
15Z	2	5.45	0.11	-1.22	-231.27	-0.32	0.13	1	2	1
16Z	2	-1.97	-0.09	-2	-12.78	-0.51	-0.03	0.11	2	1
17Z	2	-0.52	-0.01	-0.52	207.49	-0.68	-0.03	1.91	2	1
18Z	2	5.65	-0.11	-1.18	47.89	-0.67	-0.09	1.05	2	1
19Z	2	-1.66	0.2	-2.5	-123.36	-0.26	0	4.84	2	1
20Z	2	-0.11	0.25	-4.42	-219.4	0.02	0.02	4.72	1	0
21Z	2	-1.06	0.17	-2.78	-262.99	-0.29	0.12	5.99	2	1
22Z	2	-2.05	0.31	0.12	257.01	0.22	0.15	5.42	1	0
23Z	2	5.09	0.42	3.46	275.2	0	0.23	5.53	2	1
00Z	3	17.23	0.29	2.16	769.57	0.06	0.09	1.67	2	0

Table 9. The 6 meteorological parameters that were included in the neural network, in addition to, the actual and forecast class, the angle of deviation, and hits for the June 12, 2009 MCS. A hit of 1 indicates the actual and forecast track were identical while a 0 means they were different.

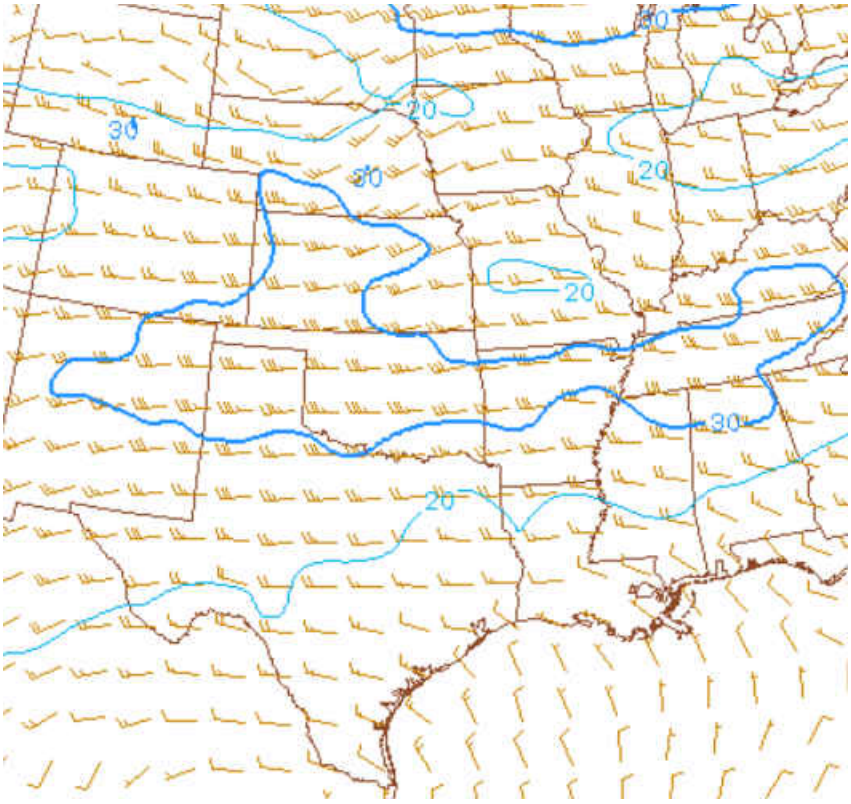

Figure 13. June 12, 2009 850-300hPa mean wind at 15 UTC.

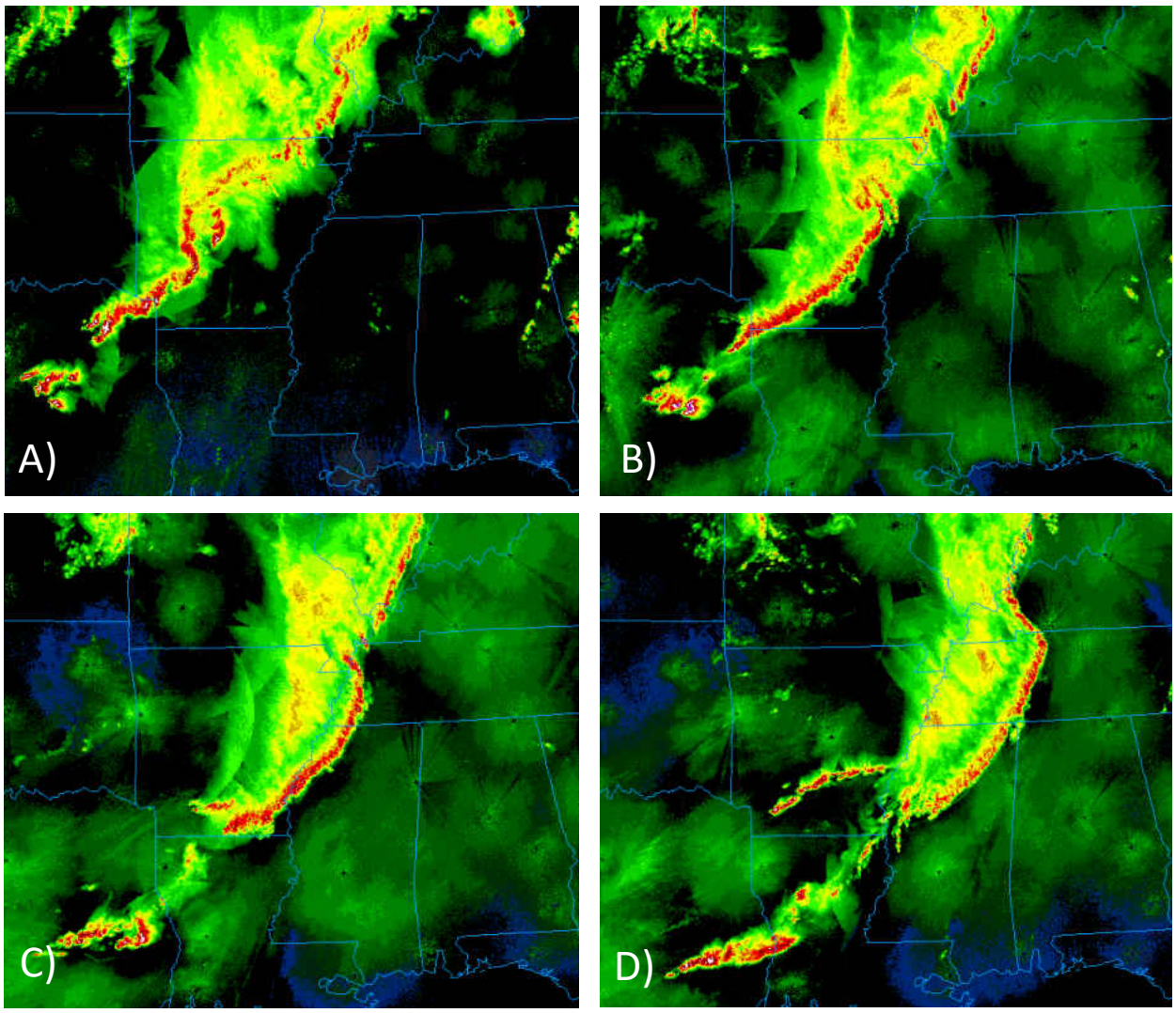

Figure 14. (a)-(d) Base reflectivity for the April 26, 2011 MCS at (a) 00 UTC, (b) 02 UTC, (c) 04 UTC, (d) 06 UTC. These were gathered from http://www2.mmm.ucar.edu/imagearchive/.

Time (UTC)	Actual Class	Degree of Deviation	700hPa Temp	Precip Water	MU CAPE	Sfc-500hPa Mean Wind	700-500hPa Lapse Rates	Theta-e Dif	Forecast Class	Hit
16Z	3	20.92	0.22	-5.82	-1164.6	-0.46	0.09	2.49	2	0
17Z	3	31.51	-0.12	-7.39	-284.39	-0.43	-0.05	6.07	3	1
18Z	3	58.76	-0.32	-9.01	332.94	-0.89	-0.13	-1.41	3	1
19Z	3	12.12	0.37	0.65	75.3	-0.9	0.26	-4.4	3	1
20Z	3	12.54	0.3	0.8	-21.64	-1.53	0	-3.75	3	1
21Z	2	-3.85	0.17	0.75	-949.57	-0.58	-0.03	-6.16	3	0

Table 10. The 6 meteorological parameters that were included in the neural network, in addition to, the actual and forecast class, the angle of deviation, and hits for the April 26, 2011 MCS. A hit of 1 indicates the actual and forecast track were identical while a 0 means they were different.

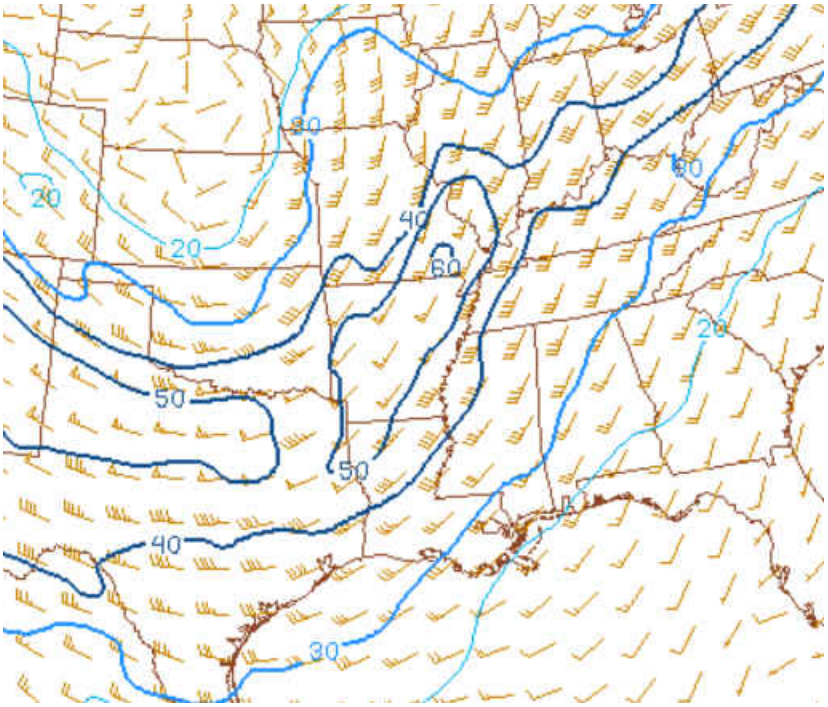

Figure 15. April 26, 2011 850-300hPa mean wind at 01 UTC.

V. REFERENCES

Banacos, P., and D. Schultz, 2005: The use of moisture flux convergence in forecasting convection initiation: Historical and operational perspectives. Wea. Forecasting, 20, 351–366.

Coniglio, M. C., H. E. Brooks, S. J. Weiss, and S. F. Corfidi, 2007: Forecasting the maintenance of quasi-linear mesoscale convective systems. *Wea. Forecasting*, **22**, 556–570.

Evans, J.S., and C.A. Doswell, 2001: Examination of derecho environments using proximity soundings. *Wea. Forecasting*, **16**, 329-342.

James, R. P., P. M. Markowski, and J. M. Fritsch, 2006: Bow echo sensitivity to ambient moisture and cold pool strength. *Mon. Wea. Rev.*, **134**, 950–964.

Johns, R. H., and W. D. Hirt, 1987: Derechos: widespread convectively induced windstorms. *Wea. Forecasting*, **2**, 32-49.

Jirak, I. L., and W. R. Cotton, 2007: Observational analysis and predictability of mesoscale convective systems. *Wea. Forecasting*, **22**, 813–838.

Merritt, J. H., and J. M. Fritsch, 1984: On the movement of the heavy precipitation areas of mid-latitude mesoscale convective complexes. Preprints, *10th Conf. on Weather Analysis and Forecasting,* Clearwater Beach, FL, Amer. Meteor. Soc., 529–536.

Roebber, P. J., S. Bruening, D. M. Schultz, and J. V. Cortinas Jr., 2003: Improving snowfall forecasting by diagnosing snow density. *Wea. Forecasting*, **18**, 264–287.

Thompson, R. L., R. Edwards, J. A. Hart, K. L. Elmore, and P. Markowski, 2003: Close proximity soundings within supercell environments obtained from the Rapid Update Cycle. *Wea. Forecasting*, **18**, 1243–1261.

VI. APPENDIX

a. Artificial Neural Network Input Node Equations

Note: Lapse_R_4 is the 700-500hPa lapse rate at point 4 (the description of numbering the points can be found in the methodology), Mean_W_6 is the surface-500hPa mean wind at point 6, Temp_700_4 is the 700hPa temperature at point 4, Precip_W_8 is the precipitable water at point 8, and the CAPE_MU_5 is the most unstable CAPE at point 5.

Node 1:
TanH(0.5 * ((-0.312998195383049) + (-0.861639799434503 * Lapse_R_4) +
(-0.0854010075421984 * Mean_W_6) + 0.177413848260043 * Temp_700_4 +
(-0.0806514109025484 * Precip_W_8) + 0.000663438005474068 * CAPE_MU_5
+0.123558427048433 * ThetaE_Dif_2))

Node 2:
TanH(0.5 * (0.383018716662308 + (-1.56999121351854 * Lapse_R_4) + 1.16517715719708 *
Mean_W_6 + (-1.04543837486005 * Temp_700_4) + 0.119230955376078 * Precip_W_8
+(-0.000779638959420064 * CAPE_MU_5) + (-0.0542058801069476 * ThetaE_Dif_2)))

Node 3:
TanH(0.5 * ((-0.186294552778093) + (-0.0470495460843277 * Lapse_R_4)
+0.667055561257761 * Mean_W_6 + 0.511011300749929 * Temp_700_4
+0.1701691560616 * Precip_W_8 + 0.000813546351020121 * CAPE_MU_5
+0.257857195872967 * ThetaE_Dif_2))

Node 4:
TanH(0.5 * ((-0.0600934641536502) + 0.0800981853601172 * Lapse_R_4 +
(-0.480270389728447 * Mean_W_6) + (-0.563610011886647 * Temp_700_4)
+0.0191958321661417 * Precip_W_8 + 0.00158976207810333 * CAPE_MU_5
+0.0205571519397239 * ThetaE_Dif_2))

Node 5:
TanH(0.5 * (0.210715537550994 + (-3.3037579744206 * Lapse_R_4) + (-1.92234749554859 *
Mean_W_6) + (-1.81077937098855 * Temp_700_4) + (-0.0406344146213817 * Precip_W_8)
+ (-0.000318656425172095 * CAPE_MU_5) + 0.0616277778551394 * ThetaE_Dif_2))

Node 6:

TanH(0.5 * (0.566241472496902 + (-2.66795414568064 * Lapse_R_4) + 0.314602205449724 * Mean_W_6 + (-2.29773087788169 * Temp_700_4) + (-0.0591218307783031 * Precip_W_8) + (-0.000809842044393637 * CAPE_MU_5) + (-0.0336908991895603 * ThetaE_Dif_2)))

Node 7:
TanH(0.5 * (0.0316268460309597 + (-1.48122424256465 * Lapse_R_4) + 0.465996790016292 * Mean_W_6 + 1.088589419108 * Temp_700_4 + (-0.0018184597043054 * Precip_W_8) + (-0.000912278243020361 * CAPE_MU_5) + (-0.000611144923158101 * ThetaE_Dif_2)))

Node 8:
TanH(0.5 * (0.148687273277041 + (-1.62562753304091 * Lapse_R_4) + (-0.283396658708113 * Mean_W_6) + (-0.555096540145314 * Temp_700_4) + (-0.148477561329891 * Precip_W_8) + 0.0000141407539487639 * CAPE_MU_5 + (-0.0227980068862207 * ThetaE_Dif_2)))

Node 9:
TanH(0.5 * (0.489575452667522 + (-2.11971030898637 * Lapse_R_4) + (-1.55942450058709 * Mean_W_6) + (-2.87096553246257 * Temp_700_4) + (-0.332167929941937 * Precip_W_8) + 0.000220485678940086 * CAPE_MU_5 + (-0.0279419457191649 * ThetaE_Dif_2)))

Node 10:
TanH(0.5 * (0.537243108135552 + (-2.67181952355903 * Lapse_R_4) + 1.20786565676066 * Mean_W_6 + (-0.416671585072205 * Temp_700_4) + (-0.024209295817086 * Precip_W_8) + 0.0000056327581337879 * CAPE_MU_5 + 0.0142685006227867 * ThetaE_Dif_2))

Node 11:
TanH(0.5 * ((-0.42254999609531) + 0.110842345928629 * Lapse_R_4 + (-1.53844826265695 * Mean_W_6) + 1.34880464199006 * Temp_700_4 + 0.229050620764187 * Precip_W_8 + 0.000113019914537344 * CAPE_MU_5 + 0.104261978711348 * ThetaE_Dif_2))

Node 12:
TanH(0.5 * ((-0.584457763284563) + 2.51342014612925 * Lapse_R_4 + (-1.21631400303524 * Mean_W_6) + 0.731219185865046 * Temp_700_4 + (-0.111530831783616 * Precip_W_8) + (-0.00127552854617491 * CAPE_MU_5) + (-0.0707438684258752 * ThetaE_Dif_2)))

Node 13:
TanH(0.5 * (0.503475255438858 + (-5.18303347553372 * Lapse_R_4) + 0.572540539257258 * Mean_W_6 + (-0.932050685394089 * Temp_700_4) + (-0.384050204468855 * Precip_W_8) + (-0.000577611854872146 * CAPE_MU_5) + 0.117398209333869 * ThetaE_Dif_2))

Node 14:
TanH(0.5 * (0.163175824147292 + 1.8349506447891 * Lapse_R_4 + 1.42270142763081 * Mean_W_6 + (-1.26721164883268 * Temp_700_4) + 0.114484115138127 * Precip_W_8

+(-0.00159681527101823 * CAPE_MU_5) + 0.0210234800054395 * ThetaE_Dif_2))

Node 15:
TanH(0.5 * ((-1.00627285132541) + 1.66933077833997 * Lapse_R_4 + (-0.31787020791916 * Mean_W_6) + 1.97422489816946 * Temp_700_4 + 0.171944191199688 * Precip_W_8 + 0.00104565302751889 * CAPE_MU_5 + (-0.101171193957345 * ThetaE_Dif_2)))

Node 16:
TanH(0.5 * ((-0.826465446872852) + 8.54478762224928 * Lapse_R_4 + (-2.30654367418613 * Mean_W_6) + 1.10196681058728 * Temp_700_4 + 0.0387464031470233 * Precip_W_8 + 0.000979891581797218 * CAPE_MU_5 + 0.0133596879350648 * ThetaE_Dif_2))

Node 17:
TanH(0.5 * ((-0.132844269500526) + 3.36238141985796 * Lapse_R_4 + (-0.18757291590434 * Mean_W_6) + (-1.01810714611921 * Temp_700_4) + (-0.0619488278162703 * Precip_W_8) + 0.000301508652212921 * CAPE_MU_5 + 0.0657979050148123 * ThetaE_Dif_2))

Node 18:
TanH(0.5 * (0.151987159218665 + (-3.750374006312 * Lapse_R_4) + (-0.364717515552427 * Mean_W_6) + (-1.12755869585317 * Temp_700_4) + 0.127794325906269 * Precip_W_8 +(-0.000443322207737791 * CAPE_MU_5) + (-0.140102638338899 * ThetaE_Dif_2)))

Node 19:
TanH(0.5 * ((-0.140702880341922) + (-0.0238085123895683 * Lapse_R_4) +0.255208568523875 * Mean_W_6 + 1.35112920571401 * Temp_700_4 + (-0.150235636163027 * Precip_W_8) + (-0.000924658951904272 * CAPE_MU_5) +0.0352787128783076 * ThetaE_Dif_2))

Node 20:
TanH(0.5 * (0.187648951167735 + (-2.91974681638891 * Lapse_R_4) + 0.103504494210068 * Mean_W_6 + (-0.545225986543171 * Temp_700_4) + (-0.00298302399092736 * Precip_W_8) + 0.000168823830861263 * CAPE_MU_5 + (-0.0900618807552676 * ThetaE_Dif_2)))

Node 21:
TanH(0.5 * (0.287769091659785 + 0.924746475018714 * Lapse_R_4 + (-2.07262749419797 * Mean_W_6) + 0.365300014743662 * Temp_700_4 + (-0.0722142421750039 * Precip_W_8) + (-0.0000282842950385927 * CAPE_MU_5) + 0.0309237570721295 * ThetaE_Dif_2))

b. *Artificial Neural Network Probability Equations for each Class*

Equation for Class 1 (Left(-Moving):

Note: H1_1 is the first node, H1_2 is the second node, and so on.

Exp(0.207527951383221 + 0.187706412677864 * H1_1 2 + (-0.152881570942793 * H1_2 2)

+ (-0.401716546254537 * H1_3 2 + (-0.789563997499046 * H1_4 2) +
(-0.854821043761416 * H1_5 2) + (-0.874866113680077 * H1_6) + 0.743118602937288 *
H1_7 + 0.247494449981411 * H1_8 + 0.759785189112915 * H1_9
+0.0781389394430124 * H1_10 + 1.19683171841811 * H1_11 + (-1.58807277127848 *
H1_12) + 1.81588500801269 * H1_13 + 0.850944364753991 * H1_14 +
(-0.499641858036212 * H1_15) + 1.6164183637284 * H1_16 + 0.104889430270215 *
H1_17 + 0.991828188256044 * H1_18 + (-0.291680322804769 * H1_19) +
(-0.0687173631533351 * H1_20) + (-1.62872485175183 * H1_21)
) / (1 + Exp(
0.207527951383221 + 0.187706412677864 * H1_1 2 + (-0.152881570942793 * H1_2 2)
+ (-0.401716546254537 * H1_3 2) + (-0.789563997499046 * H1_4 2) +
(-0.854821043761416 * H1_5 2) + (-0.874866113680077 * H1_6) + 0.743118602937288 *
H1_7 + 0.247494449981411 * H1_8 + 0.759785189112915 * H1_9
+0.0781389394430124 * H1_10 + 1.19683171841811 * H1_11 + (-1.58807277127848 *
H1_12) + 1.81588500801269 * H1_13 + 0.850944364753991 * H1_14 +
(-0.499641858036212 * H1_15) + 1.6164183637284 * H1_16 + 0.104889430270215 *
H1_17 + 0.991828188256044 * H1_18 + (-0.291680322804769 * H1_19) +
(-0.0687173631533351 * H1_20) + (-1.62872485175183 * H1_21)) + Exp(0.762584847149082 +
0.193455925501196 * H1_1 2 + 1.76846564770736 * H1_2 2
+1.20111870055491 * H1_3 2 + 0.0926587928172754 * H1_4 2 + 0.7242827544073 *
H1_5 2 + (-1.20163287947958 * H1_6) + 0.832231653576481 * H1_7
+0.273825133989891 * H1_8 + 1.289426585541 * H1_9 + (-0.202547033096641 *
H1_10) + (-0.624126056119543 * H1_11) + 0.183644303704899 * H1_12
+1.60640961889727 * H1_13 + 1.56035627546325 * H1_14 + 1.52709845990362 *
H1_15 + 1.72549755799604 * H1_16 + (-0.745702367097591 * H1_17)
+0.236942077816432 * H1_18 + (-0.786011038461368 * H1_19) + (-0.349593421930795
* H1_20) + (-0.470954274006917 * H1_21)))

Equation for Class 2 (Middle):

Exp(0.762584847149082 + 0.193455925501196 * H1_1 2 + 1.76846564770736 * H1_2 2

+1.20111870055491 * H1_3 2 + 0.0926587928172754 * H1_4 2 + 0.7242827544073 *

H1_5 2 + (-1.20163287947958 * H1_6) + 0.832231653576481 * H1_7
+0.273825133989891 * H1_8 + 1.289426585541 * H1_9 + (-0.202547033096641 *
H1_10) + (-0.624126056119543 * H1_11) + 0.183644303704899 * H1_12
+1.60640961889727 * H1_13 + 1.56035627546325 * H1_14 + 1.52709845990362 *
H1_15 + 1.72549755799604 * H1_16 + (-0.745702367097591 * H1_17)
+0.236942077816432 * H1_18 + (-0.786011038461368 * H1_19) + (-0.349593421930795
* H1_20) + (-0.470954274006917 * H1_21)
) / (1 + Exp(
0.207527951383221 + 0.187706412677864 * H1_1 2 + (-0.152881570942793 * H1_2 2)
+ (-0.401716546254537 * H1_3 2) + (-0.789563997499046 * H1_4 2) +
(-0.854821043761416 * H1_5 2) + (-0.874866113680077 * H1_6) + 0.743118602937288 *
H1_7 + 0.247494449981411 * H1_8 + 0.759785189112915 * H1_9
+0.0781389394430124 * H1_10 + 1.19683171841811 * H1_11 + (-1.58807277127848 *
H1_12) + 1.81588500801269 * H1_13 + 0.850944364753991 * H1_14 +
(-0.499641858036212 * H1_15) + 1.6164183637284 * H1_16 + 0.104889430270215 *
H1_17 + 0.991828188256044 * H1_18 + (-0.291680322804769 * H1_19) +
(-0.0687173631533351 * H1_20) + (-1.62872485175183 * H1_21)
) + Exp(
0.762584847149082 + 0.193455925501196 * H1_1 2 + 1.76846564770736 * H1_2 2
+1.20111870055491 * H1_3 2 + 0.0926587928172754 * H1_4 2 + 0.7242827544073 *
H1_5 2 + (-1.20163287947958 * H1_6) + 0.832231653576481 * H1_7
+0.273825133989891 * H1_8 + 1.289426585541 * H1_9 + (-0.202547033096641 *
H1_10) + (-0.624126056119543 * H1_11) + 0.183644303704899 * H1_12
+1.60640961889727 * H1_13 + 1.56035627546325 * H1_14 + 1.52709845990362 *
H1_15 + 1.72549755799604 * H1_16 + (-0.745702367097591 * H1_17)
+0.236942077816432 * H1_18 + (-0.786011038461368 * H1_19) + (-0.349593421930795
* H1_20) + (-0.470954274006917 * H1_21)))

Equation for Class 3 (Right(-Moving):

1 / (1 + Exp(0.207527951383221 + 0.187706412677864 * H1_1 2 + (-0.152881570942793 *
H1_2 2) + (-0.401716546254537 * H1_3 2) + (-0.789563997499046 * H1_4 2) + (-
0.854821043761416 * H1_5 2) + (-0.874866113680077 * H1_6) + 0.743118602937288 *

H1_7 + 0.247494449981411 * H1_8 + 0.759785189112915 * H1_9
+0.0781389394430124 * H1_10 + 1.19683171841811 * H1_11 + (-1.58807277127848 *
H1_12) + 1.81588500801269 * H1_13 + 0.850944364753991 * H1_14 +
(-0.499641858036212 * H1_15) + 1.6164183637284 * H1_16 + 0.104889430270215 *
H1_17 + 0.991828188256044 * H1_18 + (-0.291680322804769 * H1_19) +
(-0.0687173631533351 * H1_20) + (-1.62872485175183 * H1_21)
) + Exp(
0.762584847149082 + 0.193455925501196 * H1_1 2 + 1.76846564770736 * H1_2 2

+1.20111870055491 * H1_3 2 + 0.0926587928172754 * H1_4 2 + 0.7242827544073 * H1_5 2 + (-1.20163287947958 * H1_6) + 0.832231653576481 * H1_7 +0.273825133989891 * H1_8 + 1.289426585541 * H1_9 + (-0.202547033096641 * H1_10) + (-0.624126056119543 * H1_11) + 0.183644303704899 * H1_12 +1.60640961889727 * H1_13 + 1.56035627546325 * H1_14 + 1.52709845990362 * H1_15 + 1.72549755799604 * H1_16 + (-0.745702367097591 * H1_17) +0.236942077816432 * H1_18 + (-0.786011038461368 * H1_19) + (-0.349593421930795 * H1_20) + (-0.470954274006917 * H1_21)))